

## Ab Initio Study of M<sup>+</sup>:18-Crown-6 Microsolvation

David Feller\*

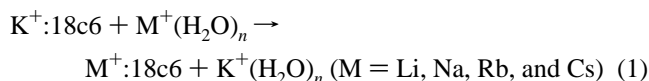
Environmental Molecular Sciences Laboratory, Pacific Northwest National Laboratory, 906 Battelle Boulevard, MS K1-90, Richland, Washington 99352

Received: December 17, 1996; In Final Form: January 28, 1997<sup>⊗</sup>

The effect of aqueous microsolvation on the relative binding affinities of 18-crown-6 for the alkali metal cations (Li<sup>+</sup>–Cs<sup>+</sup>) was studied using second-order perturbation theory and polarized basis sets augmented with diffuse functions to minimize basis set superposition error. A cation exchange reaction involving the replacement of potassium in a cation/crown complex with a different alkali cation contained within a cation/water cluster served as the basis for modeling binding preferences in liquid water. Up through four crown ether waters of solvation (six for Li<sup>+</sup> and K<sup>+</sup>) were considered, in conjunction with cation/water complexes including as many as nine waters. The principal impact of the added waters on the K<sup>+</sup> ↔ M<sup>+</sup> exchange reaction was to sharply reduce the spread in binding enthalpies among the different elements, narrowing the discrepancy between the theoretical gas phase cluster results and experimental findings obtained in aqueous solutions.

### Introduction

Crown ethers display the ability to selectively bind specific metal cations in the presence of complex aqueous mixtures of chemically similar ions. Horwitz et al.<sup>1</sup> have proposed crown ethers for separating high-level nuclear wastes such as <sup>90</sup>Sr and <sup>137</sup>Cs. In two recent theoretical studies, the gas phase binding preferences of 18-crown-6 (18c6) for alkali metal cations<sup>2</sup> and alkaline earth dications,<sup>3</sup> were computed for the first time with correlated *ab initio* techniques. Contrary to experimental observations performed in aqueous solution, where potassium and barium are the preferred species, gas phase calculations show 18c6 binds Li<sup>+</sup> and Mg<sup>2+</sup> most strongly among the two ionic sequences (Li<sup>+</sup>–Cs<sup>+</sup> and Mg<sup>2+</sup>–Ra<sup>2+</sup>) studied. By considering the ion exchange reactions,



or the analogous set of reactions for Ba<sup>2+</sup>, the aqueous phase binding preferences were qualitatively reproduced with as few as four waters of hydration. In the present work we extend the earlier study to consider the consequences of (1) increasing the number of the waters (*n*) in order to complete the first solvation shell around K<sup>+</sup> and Rb<sup>+</sup> and (2) incorporating a small number of water molecules in the metal–crown complex, i.e. microsolvating the crown. By increasing *n* we hope to determine if additional waters of hydration will significantly alter the relative reaction enthalpies for eq 1. In our earlier work, it appeared that several of the Δ*H* vs *n* curves had not converged for values of *n* ≤ 4. In solution, the cation/crown complexes would be surrounded by solvent molecules that might play a significant role in shifting the preference for one cation over another, as measured by the Δ*H* of reaction for eq 1. By considering the effects of a small number of waters bound to the M<sup>+</sup>:18c6 complex, we hope to simulate the dominant effects of directly interacting solvent molecules on the crown's binding preferences. To the best of our knowledge, this is the first attempt to apply *ab initio* techniques in the study of crown ether

microsolvation. *Ab initio* microsolvation studies are still rare due to the expense of the calculations,<sup>4</sup> but recent developments may drastically reduce the costs.<sup>5,6</sup> On the other hand, molecular dynamics simulations based on classical force fields are able to incorporate up through several hundred waters.<sup>7,8</sup>

### Procedure

The approach adopted here is the same as that used in the two previous studies. Geometries were optimized with restricted Hartree–Fock (RHF) wave functions. The 6-31+G\* polarized basis set,<sup>9–11</sup> minus the diffuse functions on carbon, was chosen, along with the Hay and Wadt<sup>12</sup> effective core potentials (ECPs) to replace the deep core electrons in K, Rb, and Cs. ECPs for the latter two elements include the dominant mass–velocity and one-electron Darwin relativistic corrections. The electrons in the metal (*n*–1) shell, e.g. the (3s,3p) shell in K or the (4s,4p) shell in Rb, were treated explicitly and included in the correlation treatment.

The valence basis sets for K, Rb, and Cs were taken from Hay and Wadt.<sup>12</sup> Polarization exponents (ζ<sub>Kd</sub> = 0.48, ζ<sub>Rbd</sub> = 0.24, and ζ<sub>Csd</sub> = 0.19) were taken from the earlier work.<sup>2</sup> Enthalpy corrections to the crown's electronic binding energies were determined with scaled RHF/3-21G frequencies (scale factor = 0.9). All calculations were performed with the Gaussian 94<sup>13</sup> program. Six-component Cartesian d functions were used. Geometries were optimized with the “tight” gradient convergence threshold, except where noted. In a few cases Gaussian appeared unable to reduce the gradient to this level despite hundreds of steps. Since total energies appeared converged beyond 10<sup>–6</sup> E<sub>h</sub> and metal–oxygen distances were varying by less than 10<sup>–3</sup> Å, the calculations were halted. Details of the basis sets, ECPs, and all optimized geometries are available from the author upon request.

Binding energies were also evaluated with second-order Møller–Plesset perturbation theory (MP2) and corrected for the effects of basis set superposition error (BSSE) with the full Boys–Bernardi counterpoise (CP) procedure.<sup>14</sup> A recent article by Xantheas<sup>15</sup> has stressed the importance of using fragment geometries taken from the optimized “AB” complex when computing this correction. In the present work, as well as in all of our previous work, CP corrections were computed with the so-called “relaxed” fragment geometries.

\* E-mail: d3e102@ames.pnl.gov. Fax: (509)-375-6631.

⊗ Abstract published in *Advance ACS Abstracts*, March 15, 1997.

Comparisons of the computational approach adopted here with much larger basis set calculations and more extensive correlation recovery (e.g. fourth-order Møller–Plesset perturbation theory and coupled cluster theory) suggest that MP2/6-31+G\*(CP) binding energies are typically within  $\pm 2$  kcal/mol of the best theoretical binding energies available.<sup>16</sup> Although  $M^+(H_2O)_n$  ( $n \geq 6$ ) water–water distances predicted at the RHF/6-31+G\* level of theory are known to differ from those obtained at higher levels of theory by as much as 0.1 Å, the energetic consequences of this error are small due to the weakness of the hydrogen bonds.<sup>17,18</sup> A recent study of cation–ether binding energies evaluated at RHF and MP2 geometries has shown that the added expense of performing MP2 geometry optimization is unwarranted for these complexes, unless very high levels of accuracy are sought.<sup>19</sup>

### $M^+(H_2O)_n$ ( $n = 7-9$ )

We have previously reported RHF/6-31+G\* structures and binding enthalpies at 298 K for  $M^+(H_2O)_n$  clusters ( $n = 1-6$ ,  $M = Li, Na, K, Rb,$  and  $Cs$ ).<sup>18,20</sup> A subsequent study extended this work up through  $n = 9$  for  $Na^+$  and  $K^+$ .<sup>19</sup> The two practical obstacles to performing accurate cluster calculations with larger numbers of waters are (1) the rapidly increasing number of low-lying conformations within 5 kcal/mol of the global minimum as  $n$  increases and (2) the lack of ECP analytical second derivatives in Gaussian 94, resulting in very long normal mode calculations. Several recent reports<sup>21-23</sup> of pure water clusters with  $n \leq 9$  illustrate the magnitude of the first problem. Dozens of structures were identified within 10 kcal/mol of the global minimum. Fortunately, the presence of a cation appears to reduce the number of low-lying conformations in cation/water clusters, at least for  $n$  smaller than the number required to fill the first solvation shell, because of the directional nature of the strong charge–dipole interaction. Nonetheless, the existence of multiple minima complicates the identification of the global minimum's geometry and, to a lesser extent, its energy.

Since the focus of the present work is the effect of added waters on relative binding energies, the consequences of failing to identify the true global minimum is less important. For example, the lowest energy conformation for sodium and six waters found in our previous study was a “4+2 ( $C_2$ )” structure, where the notation “ $m+n$ ” indicates the number of waters in the first ( $m$ ) and second ( $n$ ) solvation shells. However, subsequent calculations at the same level of theory uncovered a  $D_{2d}$  conformation with a total binding enthalpy several kcal/mol more stable (see Figure 1). Changes in basis set or level of theory may well lead to slightly different orderings. Candidates for the global minimum were obtained from a combination of chemical intuition and classical molecular dynamics. Despite examining many different conformations, there is no guarantee that the global minimum was located in all cases. As a consequence, a conservative analysis suggests an inherent uncertainty on the order of  $\pm 2$  kcal/mol in our cation/water binding enthalpies.

Due to its small ionic radius, lithium presented something of a special case. Our search for low-lying conformations of  $Li^+(H_2O)_7$  identified the structure in Figure 2 as the lowest energy form. The seventh water has begun to fill in the third solvation shell, whereas for the larger cations the seventh through ninth waters are still completing the first or second shells. Lithium also displayed the least favorable energetics in the  $K^+ \leftrightarrow M^+$  exchange reaction (1). As a result, no search was conducted for lithium/water clusters with more than seven waters.

Figure 3 shows the lowest energy conformations of  $M^+(H_2O)_n$  ( $n = 7-9$ ,  $M = Na^+, K^+, Rb^+,$  and  $Cs^+$ ) identified at the RHF/

### $Na^+(H_2O)_6$ RHF/6-31+G\* Geometries

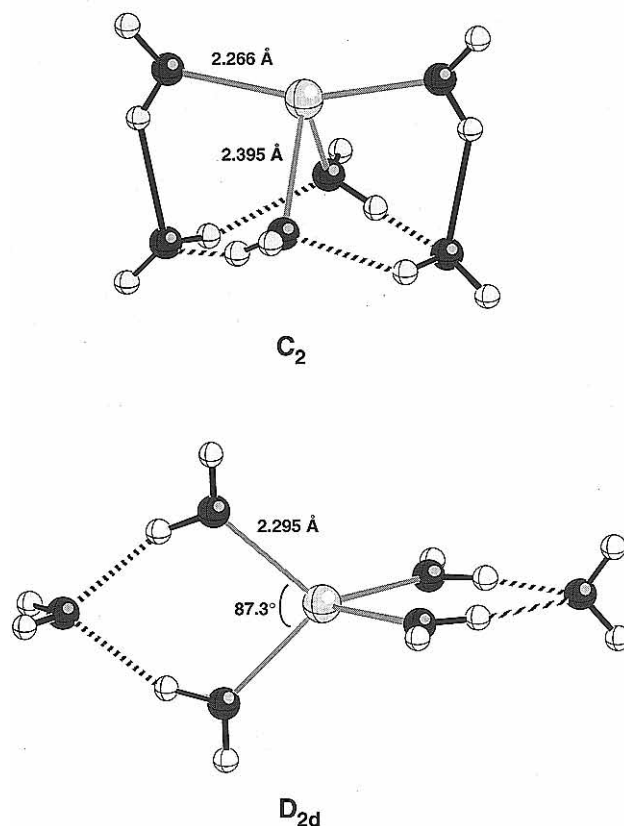


**Figure 1.** RHF/6-31+G\* hybrid basis set optimal geometries for  $Na^+(H_2O)_6$ . The total binding enthalpy (298 K) of the  $D_{2d}$  structure is 2.2 kcal/mol larger than the  $C_2$  structure.

### $Li^+(H_2O)_7$ RHF/6-31+G\* Geometry

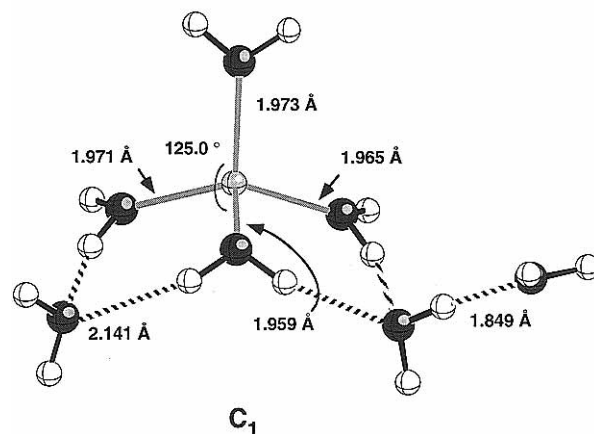


**Figure 2.** RHF/6-31+G\* optimized geometry for  $Li^+(H_2O)_7$ .

6-31+G\* level of theory. With the exception of sodium, all of the  $n = 7$  clusters consist of a cation sandwiched between three- and four-member rings that exhibit cooperative hydrogen bonding networks among the waters, while simultaneously permitting the oxygens to approach as closely as possible to the cation. The  $K^+, Rb^+,$  and  $Cs^+$   $n = 8$  complexes display approximate  $S_4$  symmetry.

For all of the  $n = 9$  complexes, the lowest energy conformation is one in which the ninth water either begins or extends the second solvation shell (see Figure 3), but the energy

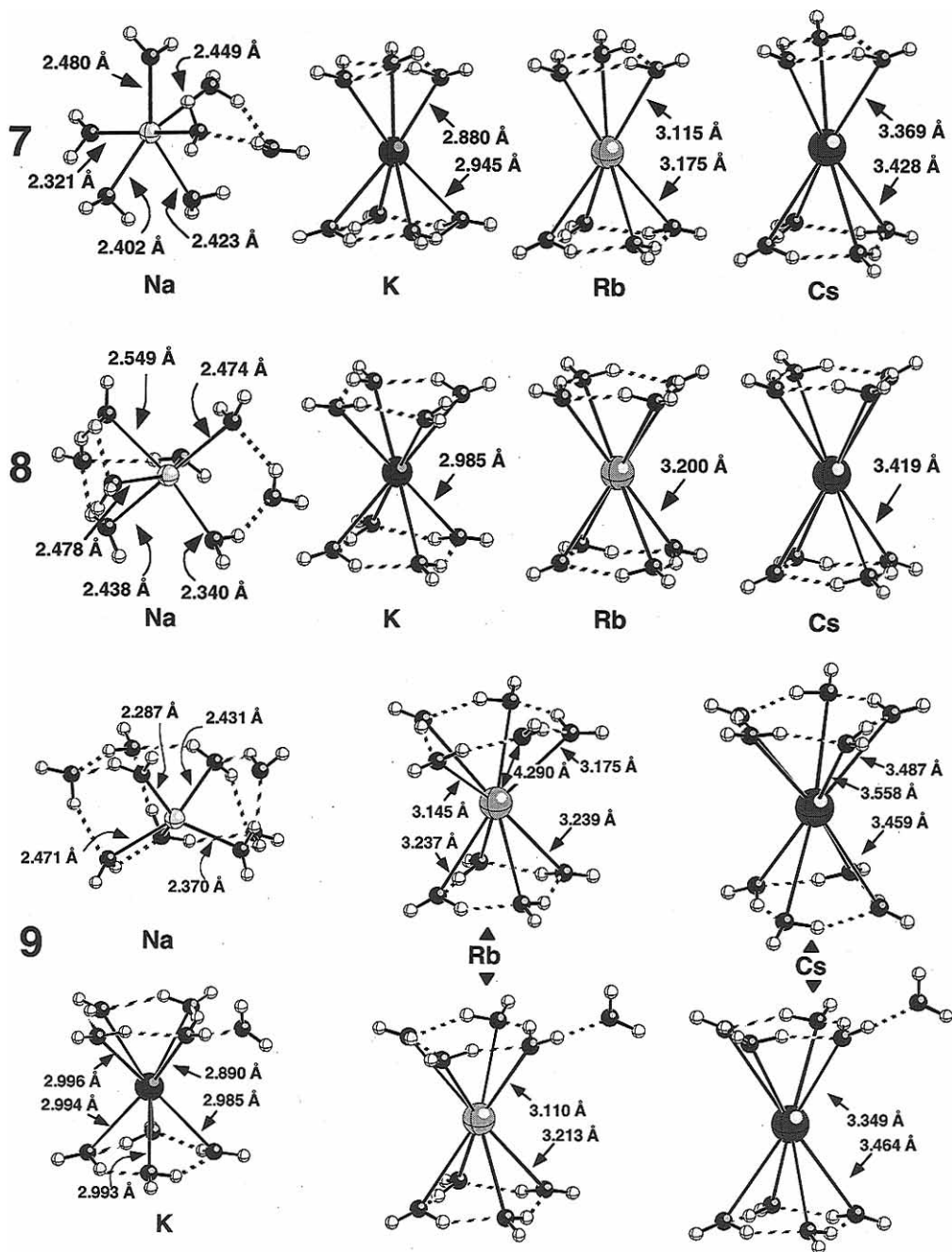


**Figure 3.** Selected RHF/6-31+G\* optimized geometries for  $M^+(H_2O)_n$ ,  $n = 7-9$ ,  $M = Na, K, Rb$ , and  $Cs$ .

difference between this structure and one in which the ninth water bonds directly to the cation is only  $\sim 1$  kcal/mol at the counterpoise-corrected MP2 level. Without the correction for BSSE, the orderings are actually reversed.

Energies and total binding enthalpies, corresponding to the complete dissociation into cation and  $n$  waters ( $M^+ + n(H_2O) \rightarrow M^+(H_2O)_n$ ), are listed in Table 1 for the newly identified cation/water clusters. The correlation correction to the binding enthalpy, which for a single water is less than 1 kcal/mol with the 6-31+G\* basis set, grows monotonically with the increasing size of the clusters to a value of 9 kcal/mol for the  $M^+(H_2O)_9$  clusters. This increase results from the increasing dominance of correlation contributions to  $\Delta H$  from hydrogen bonds. Hartree-Fock theory underestimates the water-water interaction by 0.5 kcal/mol per bond with the 6-31G\* basis set, compared to the best available theoretical estimates.<sup>24-26</sup>

By combining the present results with literature values<sup>20</sup> for smaller clusters, we were able to obtain incremental binding

enthalpies up through  $n = 9$  (see Figure 4). Although the available experimental values from Dzidic and Kebarle<sup>27</sup> and Rogers and Armentrout<sup>28</sup> extend only through  $n = 6$ , the overall level of agreement between theory and experiment is very good, but several cases, e.g. the  $Rb^+(H_2O)_2$  and  $Cs^+(H_2O)_2$  clusters, exhibit larger than normal errors for reasons that are not clear. A similar pattern was observed in two joint theoretical/experimental studies<sup>29,30</sup> of cation-ether clusters. The disagreement between theory and experiment for larger, multidentate ligands was sometimes significant and of unpredictable sign. Calculations with more extended basis sets have failed to reduce the margin of error. As already noted, counterpoise-corrected MP2/6-31+G\* binding enthalpies generally compare very well to results obtained from much larger basis sets. For example, as seen in Figure 4, the best available correlation consistent aug-cc-pVxZ results are within several kcal/mol of the smaller 6-31+G\* basis set binding enthalpies.

The variation in  $\Delta H(298\text{ K})$  for eq 1 as a function of  $n$ , the

**TABLE 1: RHF and MP2 Total Energies, Counterpoise-Corrected Total Binding Energies, and Enthalpies for  $M^+(H_2O)_n$ ,  $n = 7-9$  Obtained with the 6-31+G\* Hybrid Basis Set<sup>a</sup>**

	$n$	sym	no. functions	level	$E$ ( $E_h$ )	$\Delta E$ (CP) <sup>b</sup>	$\Delta H^{298}$ (CP)
Li	7	$C_1$	180	RHF	-539.5966	-139.1	-128.0
		$C_1$		MP2	-540.9526	-141.3	-130.3
Na	7	$C_1$	184	RHF	-693.9762	-112.5	-101.8
		$C_1$		MP2	-695.3430	-118.5	-107.8
8	$C_1$	207	RHF	-770.0101	-119.6	-106.8	
			$C_1$	MP2	-771.5749	-126.1	-113.2
9	$C_1$	230	RHF	-846.0472	-129.3	-112.5	
			$C_1$	MP2	-847.8092	-138.2	-120.8
K	7	$C_1$	176	RHF/ECP	-559.9853	-92.4	-81.6
				MP2/ECP	-561.4206	-100.1	-89.3
	8	$S_4$	199	RHF/ECP	-636.0215	-102.2	-89.6
				MP2/ECP	-637.6532	-111.5	-98.8
9	$C_1$	222	RHF/ECP	-712.0545	-110.6	-93.9	
			MP2/ECP	-713.8805	-120.8	-104.1	
Rb	7	$C_1$	176	RHF/ECP	-555.7106	-84.3	-74.2
				MP2/ECP	-557.1059	-92.2	-82.0
	8	$S_4$	199	RHF/ECP	-631.7477	-94.8	-82.9
				MP2/ECP	-633.3393	-104.3	-92.3
9	$C_1$	222	RHF/ECP	-707.7803	-103.8	-87.1	
			MP2/ECP	-709.5662	-115.2	-98.4	
Cs	7	$C_1$	176	RHF/ECP	-707.7811	-102.4	-85.5
				MP2/ECP	-709.5677	-113.2	-96.3
	8	$S_4$	199	RHF/ECP	-551.7350	-77.2	-67.0
				MP2/ECP	-553.1346	-85.7	-75.4
9	$C_1$	222	RHF/ECP	-627.7724	-87.8	-75.8	
			MP2/ECP	-629.3685	-97.8	-85.9	
$C_1^c$	$C_1$	222	RHF/ECP	-703.8045	-99.6	-83.7	
			MP2/ECP	-705.5950	-108.7	-92.8	
	$C_1^b$	$C_1$	222	RHF/ECP	-703.8056	-96.2	-80.3
				MP2/ECP	-705.5965	-107.4	-91.5

<sup>a</sup> Total energies are in hartrees. Binding energies and enthalpies are in kcal/mol. The sodium 1s electrons were treated as core. The potassium (1s,2s,2p) electrons were replaced by an effective core potential, as was the argon core for Rb and the krypton core for Cs. All calculations were performed at the optimal RHF geometries. <sup>b</sup> This structure consists of a five-membered ring and a four-membered ring capping the two ends of the cation.

number of waters in the cation/water clusters, is shown in Figure 5. In the earlier crown ether study<sup>2</sup> it was observed that a small number of waters was sufficient to recover qualitative agreement with aqueous phase binding enthalpies. This conclusion was based on values of  $n \leq 4$ . The current calculations provide no data to invalidate the original conclusion, although fluctuations in specific curves caused by differences in the relative importance of a given water molecule cause some reordering of the binding preferences. The Na curve in particular shows a  $\pm 4$  kcal/mol from  $n = 5$  to 9 as K completes its first solvation shell and begins to fill in the second shell. Because Rb and Cs are also starting to fill their second shells, the change in the Rb and Cs curves from  $n = 8$  to 9 is much smaller.

### $M^+:18c6(H_2O)_n$ ( $n = 1, 2, \text{ and } 4$ )

Optimized RHF/6-31+G\* geometries for the  $M^+:18c6$  complexes containing up to two additional waters are shown in Figures 6 and 7. In the case of the smaller cations ( $Li^+$ ,  $Na^+$ , and  $K^+$ ) the  $M^+-O_{H_2O}$  bond forms an acute angle with the mean plane of the ether oxygens, allowing the water molecule to hydrogen bond to one of the crown macrocycle oxygens. The  $Rb^+$  and  $Cs^+$  cations are too large to fit in the cavity of the crown, causing the  $M^+-O_{H_2O}$  bond to form a right angle with the plane of the crown.

Structural changes to  $K^+:18c6$  resulting from the added water were primarily localized to the macrocycle oxygen involved in the hydrogen bond. For example, all of the  $M^+-O_{macro}$

### Incremental Binding Enthalpies (298 K) $M^+(H_2O)_{n-1} \rightarrow M^+(H_2O)_n$

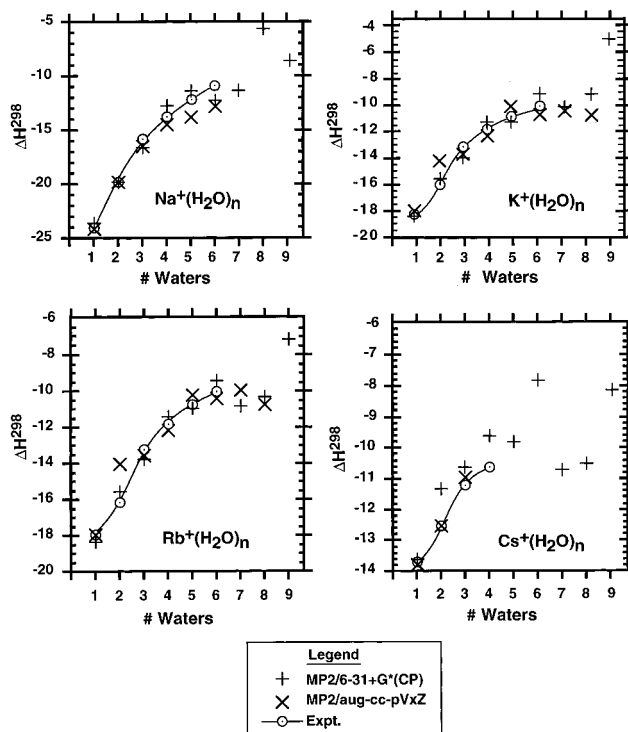


**Figure 4.** Comparison of the incremental binding enthalpy (kcal/mol) obtained from MP2/6-31+G\* and MP2/aug-cc-pVDZ theory and experiment.

### 18-crown-6 Cation Exchange Reaction Enthalpies

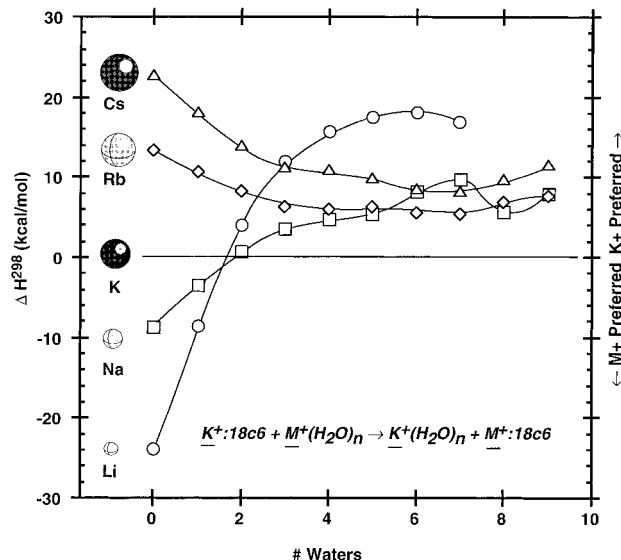


**Figure 5.** Enthalpy change for the cation exchange reaction  $K^+:18c6 + M^+(H_2O)_n \rightarrow M^+:18c6 + K^+(H_2O)_n$  ( $M = Li, Na, Rb, \text{ and } Cs$ ) at the MP2/6-31+G\* level.

distances in  $K^+:18c6$  are 2.808 Å, whereas the  $M^+-O_{macro}$  distance to the ether oxygen participating in the hydrogen bond has lengthened to 2.920 Å. Distances to the other ether oxygens have also lengthened, but by a much smaller amount (0.02 Å). The structural changes in the  $Rb^+$  and  $Cs^+$  complexes were small.

On the other hand, the lithium and sodium 18c6 complexes underwent significant changes as a result of the additional waters. In the absence of the waters, the crowns were partially

$M^+ : 18\text{-crown-6}(\text{H}_2\text{O})$  Geometries

RHF/6-31+G\* hybrid

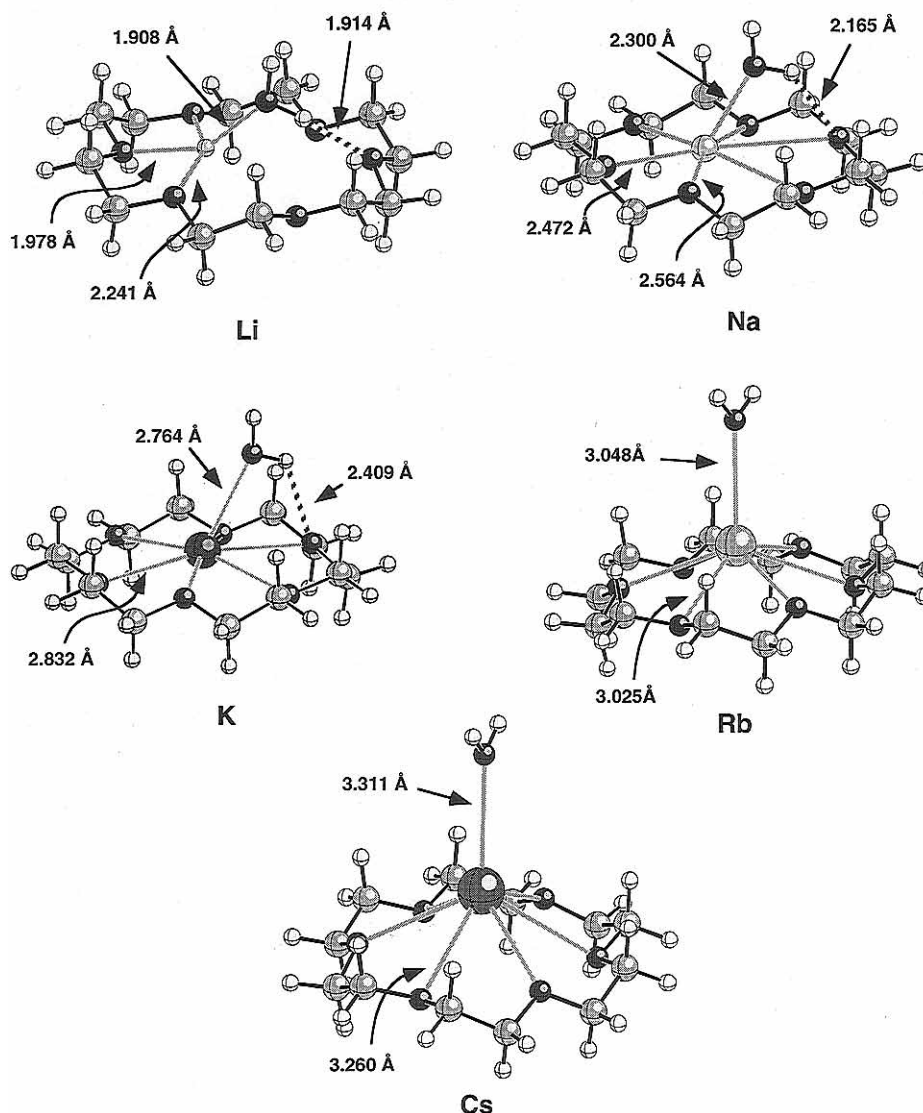


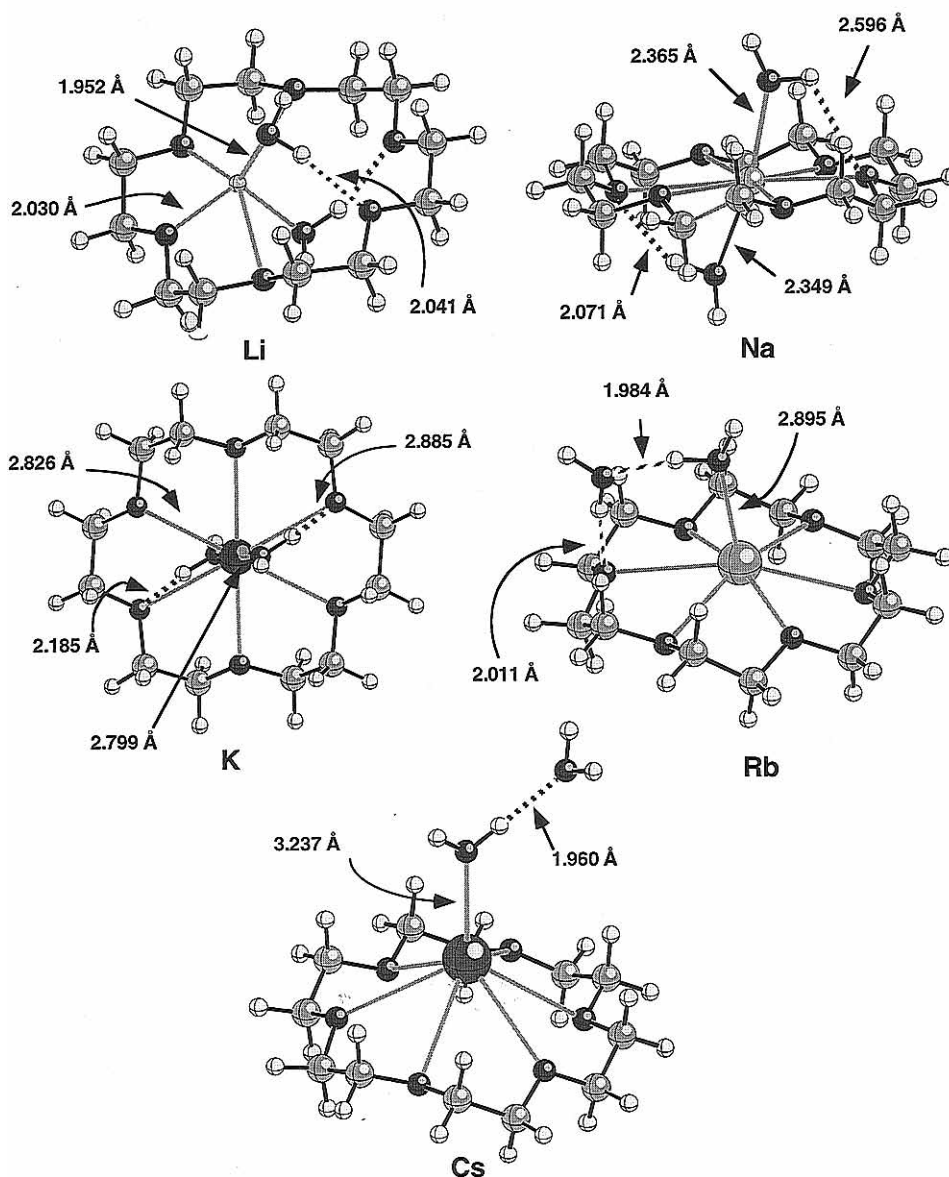
Figure 6. RHF/6-31+G\* hybrid basis set optimized for the  $M^+ : 18\text{c6}(\text{H}_2\text{O})$  complexes.

wrapped around the cation, in order to maximize the favorable electrostatic interactions between the cation and the ether oxygens. In the presence of the waters, the crown unfolds itself, assuming a more nearly planar configuration, with the metal cation positioned asymmetrically in the cavity. The water-water hydrogen bond strength at the RHF/6-31+G\* level of theory is  $-5.4$  kcal/mol, without correcting for BSSE. The energy difference between the  $S_6$  (wrapped) and  $D_{3d}$  (planar) forms of  $\text{Li}^+ : 18\text{c6}$  is  $4.6$  kcal/mol at the same level of theory. Thus, the ability to form a hydrogen bond because of the presence of the added water is more than sufficient to compensate for the energy cost of unwrapping the crown.

For the smaller cations ( $\text{Li}^+$ ,  $\text{Na}^+$ , and  $\text{K}^+$ ), the distance between the metal cation and the water oxygen,  $R(M^+ - \text{O}_{\text{H}_2\text{O}})$ , is considerably shorter than the distance between the cation and the macrocycle oxygens,  $R(M^+ - \text{O}_{\text{macro}})$ , because their ionic radii are smaller than the dimensions of the  $18\text{c6}$  cavity. By pulling the waters closer to the cation, the complex is able to maximize electrostatic attractions without the need to distort the macrocycle and increase the strain energy. For  $\text{Rb}^+$  and  $\text{Cs}^+$  the

opposite is true, i.e.  $R(M^+ - \text{O}_{\text{H}_2\text{O}}) > R(M^+ - \text{O}_{\text{macro}})$  because the cavity is too small for the cations.

Configurations with both waters on the same side of the crown, as well as configurations with waters on opposite sides, were considered for  $M^+ : 18\text{c6}(\text{H}_2\text{O})_2$ . In the case of the smaller cations, the lowest energy form was found to be one in which the waters are positioned on opposite sides, although the energy difference is small (only  $\sim 1$  kcal/mol at the MP2 level). In either case, both waters form hydrogen bonds to one of the macrocycle oxygens. For the larger cations ( $\text{Rb}$  and  $\text{Cs}$ ) both waters prefer to add to the same side in order to avoid the energy cost associated with trying to force the cation closer to the center of the crown pocket. In the  $\text{Rb}^+ : 18\text{c6}(\text{H}_2\text{O})_2$  complex the second water is sufficiently close to the crown that it can form a hydrogen bond, whereas in the case of  $\text{Cs}^+ : 18\text{c6}(\text{H}_2\text{O})_2$  the cation is sufficiently displaced from the center of mass of the crown that the second water is too far away to hydrogen bond to the ring. The form of  $\text{Cs}^+ : 18\text{c6}(\text{H}_2\text{O})_2$  in which the waters are on opposite sides of the crown lies  $18$  kcal/mol higher in energy. All attempts to locate a conformation with both water

**M<sup>+</sup>:18-crown-6(H<sub>2</sub>O)<sub>2</sub> Geometries****RHF 31+G\* hybrid**

**Figure 7.** RHF/6-31+G\* hybrid basis set optimized for the M<sup>+</sup>:18c6(H<sub>2</sub>O)<sub>2</sub> complexes.

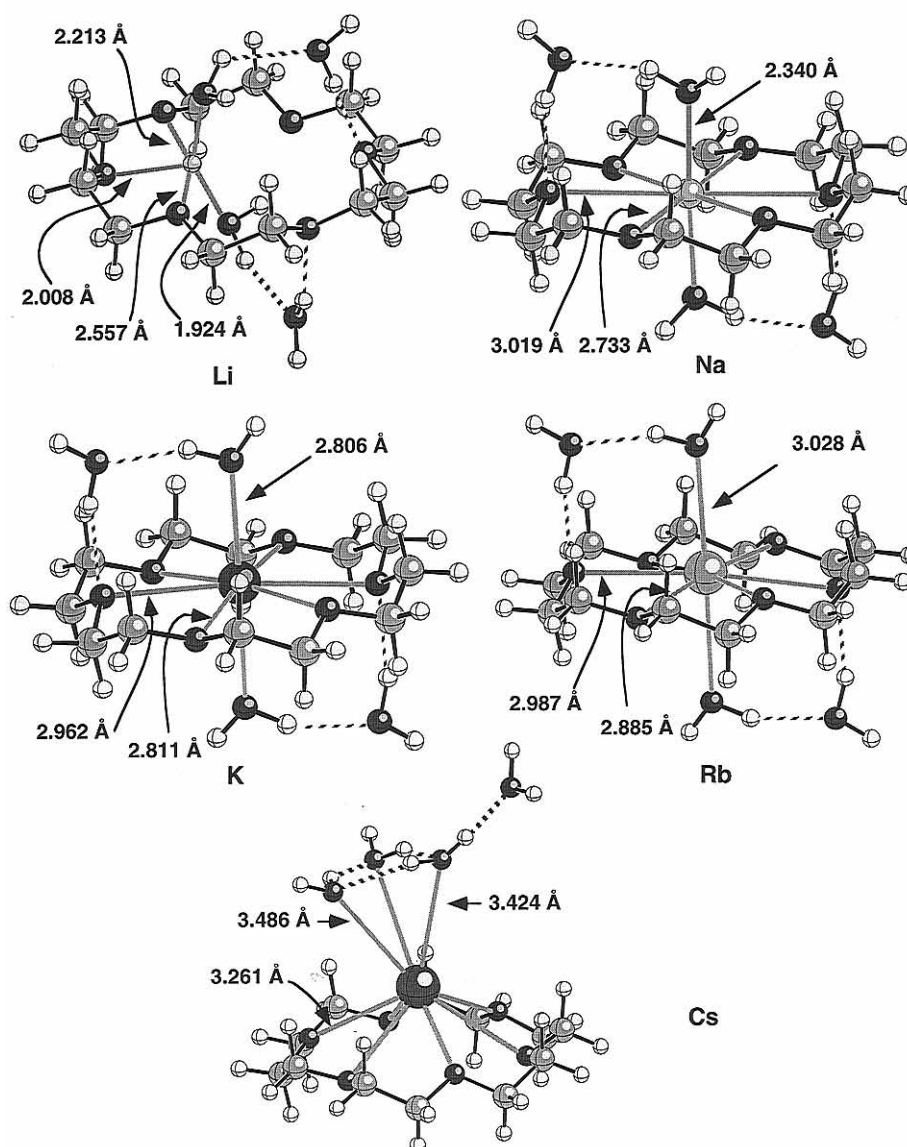
molecules directly attached to the metal cation failed, as the structures always reverted to the form show in Figure 7.

The M<sup>+</sup>:18c6(H<sub>2</sub>O)<sub>4</sub> optimized structures obtained at the RHF/6-31+G\* level of theory are shown in Figure 8. For Li through Rb, the lowest energy conformations were ones in which the waters distributed themselves evenly between the top and bottom sides of the crown. As in the case with two waters, lithium prefers to occupy an asymmetric site in the crown cavity with a closest approach to the macrocycle of ~2.01 Å. The presence of the third and fourth waters allows the directly bonded waters to adopt a more nearly orthogonal orientation to the crown ether plane. Compared to the structures with only two waters, the cation/crown portions of Na<sup>+</sup>:18c6(H<sub>2</sub>O)<sub>4</sub> and K<sup>+</sup>:18c6(H<sub>2</sub>O)<sub>4</sub> display only small structural changes. Rubidium is displaced ~0.1 Å from the mean plane of the 18c6 fragment, compared to a displacement of ~0.9 Å in the absence of the microsolvating waters.

We examined two conformations of Cs<sup>+</sup>:18c6(H<sub>2</sub>O)<sub>4</sub>. The first one resembled the Rb<sup>+</sup>:18c6(H<sub>2</sub>O)<sub>4</sub> complex shown in

Figure 8 with the cation occupying a position near the approximate center of the crown. The strength of the hydrogen bonds to the macrocyclic ethers and the Cs<sup>+</sup>-O<sub>H<sub>2</sub>O</sub> bonds are sufficient to partially offset the increased strain energy caused by squeezing the cation inside the crown cavity, unlike Cs<sup>+</sup>:18c6(H<sub>2</sub>O)<sub>2</sub>, where no minimum could be found with waters on either side of the crown. In the second configuration all four waters were positioned on the same side of the complex as the cation (see Figure 8). Three of the waters adopt a trimer configuration and are directly bonded to the cation. Because of reduced strain energy, the latter conformation was 12 kcal/mol lower in energy.

Total binding energies and enthalpies at 298 K for the M<sup>+</sup>:18c6(H<sub>2</sub>O)<sub>4</sub> complexes are listed in Table 2. MP2 increases the magnitude of the binding energies (relative to RHF) by somewhere between 4 kcal/mol (Li<sup>+</sup>) and as much as 12 kcal/mol (Cs<sup>+</sup>). The Δ*H*<sub>rxn</sub> curves for the microsolvated cation exchange reaction (Figure 9) show that the principal effect of additional waters on the crown's binding preferences is a

$M^+$ :18-crown-6( $H_2O$ )<sub>4</sub> Geometries

**Figure 8.** RHF/6-31+G\* hybrid basis set optimized for the  $M^+$ :18c6( $H_2O$ )<sub>4</sub> complexes.

pronounced reduction in the overall spread of binding enthalpies, bringing the theoretical cluster results into better accord with what is observed in aqueous solution. With just four waters, the level of agreement with the aqueous data is significantly improved. Considering the limited number of microsolvating waters and the size of the  $n = 2 \rightarrow n = 4$  change for Rb and Cs, the level of agreement with aqueous  $\Delta H$  results is probably fortuitous. Furthermore, the actual binding affinities in solution are also affected by entropic effects that are completely lacking in the present work. As we noted previously,<sup>2</sup> the large number of small frequency normal modes that are characteristic of 18c6 make it very difficult to obtain accurate entropies for these systems using our current computational approach. To include such effects for chemical systems as floppy as 18c6, researchers have carried out classical<sup>8</sup> and hybrid classical/quantum mechanical (QM/MM)<sup>31</sup> molecular dynamics simulations with several hundred waters. In either approach, the results of *ab initio* calculations are important for augmenting whatever experimental information is available. For example, in a recent QM/MM study<sup>31</sup> of 18c6 the AM1 semiempirical parameters were adjusted so as to bring the model Hamiltonian into better agreement with *ab initio* results.

The qualitative trends in  $\Delta H_{\text{rxn}}$  can be understood in terms of the three dominant contributions to the stability of the  $M^+$ :18c6( $H_2O$ )<sub>n</sub> complexes: (1) the charge-charge and charge-dipole electrostatic interactions between the positively charged metal ion and the partial negative charges on the ether oxygens and the oxygens in the microsolvating waters, (2) the strain energy of the crown, and (3) the number of hydrogen bonds. The fundamental  $M^+-O_{H_2O}$  interaction decreases monotonically from  $Li^+$  to  $Cs^+$ , paralleling the increase in the  $M^+-O_{H_2O}$  distance. The strength of the  $Cs^+(H_2O)$  bond (-14 kcal/mol) is roughly one third as strong as the bond in  $Li^+(H_2O)$ . However, the slope of the  $\Delta H_{\text{binding}}$  vs  $Z_{\text{nuc}}$  curve decreases as you progress from Li to Cs, so that the differences in binding energies are much greater for the smaller cations than the larger ones. Thus, the addition of waters that can directly bind to the  $M^+$ :18c6 complex's cation should preferentially stabilize the small alkali metals, relative to K, and slightly destabilize the complexes containing Rb and Cs.

The 18c6 strain energies, defined as the difference in energy between the crown macrocycle (with cation and waters removed) in the  $M^+$ :18c6( $H_2O$ )<sub>n</sub> complexes and the  $C_i$  global minimum, are shown in Figure 10 as a function of the number of

**TABLE 2: MP2 Total Energies, Counterpoise-Corrected Total Binding Energies, and Enthalpies for  $M^+ : 18c6(H_2O)_n$ ,  $n = 0-4$  Obtained with the 6-31+G\* Hybrid Basis Set<sup>a</sup>**

	<i>n</i>	ECP core	no. functions	<i>E</i> ( <i>E<sub>h</sub></i> )	$\Delta E$ (CP)	$\Delta H^{298}$ (CP)	
Li	0	none	361	-927.5343	-97.5	-95.4	
	1	none	384	-1003.7693	-112.3	-108.7	
	2	none	407	-1080.0200	-131.2	-125.1	
	4	none	453	-1232.4680	-145.2	-135.4	
	6	none	499	-1381.0975 <sup>b</sup>			
	Na	0	none	365	-1081.9380	-80.9	-80.3
1		none	388	-1158.1712	-95.0	-92.5	
2		none	411	-1234.4032	-104.7	-99.6	
4		none	457	-1386.8604	-115.1	-105.8	
6		Ne atom	357	-948.0275	-72.0	-71.5	
K		1	Ne atom	380	-1024.2568	-81.8	-79.5
	2	Ne atom	403	-1100.4857	-90.2	-86.2	
	4	Ne atom	449	-1252.9388	-100.6	-92.1	
	6	Ne atom	495	-1401.4969 <sup>b</sup>			
	Rb	0	Ar atom	357	-943.7064	-59.2	-58.1
		1	Ar atom	380	-1019.9311	-68.4	-66.3
2		Ar atom	403	-1096.1615	-76.1	-72.1	
4		Ar atom	449	-1248.6122	-90.9	-82.9	
Cs		0	Kr atom	357	-939.7306	-49.6	-48.7
		1	Kr atom	380	-1015.9534	-57.9	-57.2
	2	Kr atom	403	-1092.1797	-66.8	-63.6	
	4	Kr atom	449	-1244.6369	-85.9	-78.1	

<sup>a</sup> Total energies are in hartrees. Binding energies and enthalpies are in kcal/mol. <sup>b</sup> RHF energy. See text for explanation.

### The Effect of Microsolvation on 18c6

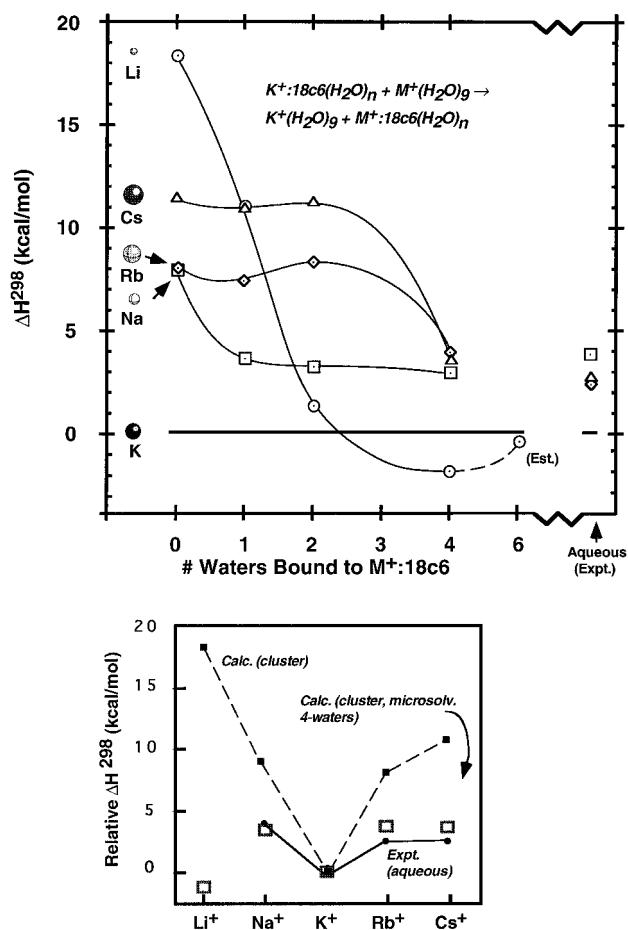


**Figure 9.** Effect of microsolvating waters on  $\Delta H_{rxn}$  for the cation exchange reaction at the MP2/6-31+G\* level. The  $Li^+ : 18c6(H_2O)_6$  data point was estimated from RHF energies, as explained in the text.

microsolvating waters. For the two smallest cations, the strain energy is of the same order of magnitude as the  $M^+(H_2O)$  bond,

### 18-crown-6 Strain Energy at the MP2/6-31+G\* Level

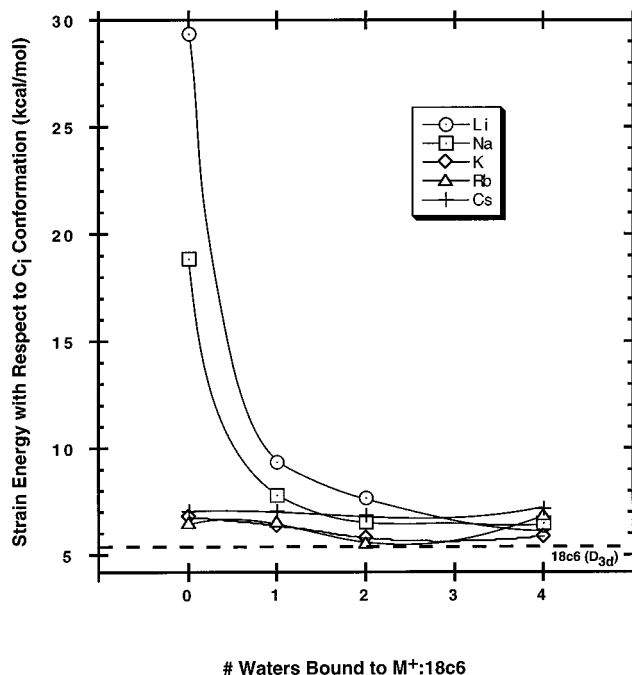


**Figure 10.** 18-Crown-6 strain energies, relative to the  $C_i$  global minimum, at the MP2/6-31+G\* level.

whereas for the larger cations it is only slightly larger than the residual 5.5 kcal/mol strain in  $D_{3d}$  18c6. The combination of reduced strain energy and strongly attractive cation–water interactions reinforce each other to produce a sharp drop in  $\Delta H$  with the first two microsolvating waters, whereas the rubidium and cesium curves in Figure 9 show essentially no change through  $n = 2$ .

The third and fourth microsolvating waters form hydrogen bonds to the macrocycle and to the first two waters. The additional waters produce very little differential effect on Na and K, as seen in Figure 9. However, the Rb and Cs complexes are further stabilized by 5–9 kcal/mol. With the exception of the distance between the metal and the directly bonded waters, the  $K^+ : 18c6(H_2O)_4$  and  $Rb^+ : 18c6(H_2O)_4$  structures are nearly identical, but Rb is 50% more polarizable, leading to a more favorable electrostatic interaction than for K. In the same vein, cesium is nearly 3 times as polarizable as potassium and the  $Cs^+ : 18c6(H_2O)_4$  complex contains a third metal–water bond.

Lithium undergoes the most dramatic change in  $\Delta H$  as a function of the degree of microsolvation. With four waters, lithium is predicted to be favored over potassium by 2 kcal/mol. Direct comparison with experiment isn't possible, as we know of no experimental measurements of  $\Delta H_{aqueous}$  for lithium. The binding constant has been estimated to be near zero,<sup>32</sup> but without information on the size of the entropy contribution to  $\Delta G$ , it is impossible to draw conclusions about the enthalpy component. Because of the large changes in  $\Delta H$  with up to four waters, it would clearly be desirable to determine the effects of including even more waters in our calculations. However, counterpoise-corrected MP2 calculations on  $M^+ : 18c6(H_2O)_n$  ( $n > 4$ ) complexes were considered prohibitively expensive. Nevertheless, we estimated  $\Delta H_{MP2}$  by performing RHF geometry optimizations on  $Li^+ : 18c6(H_2O)_6$  and  $K^+ : 18c6(H_2O)_6$  with a loose convergence criterion ( $\sim 0.0001 E_h$  in total energy). The RHF energies were adjusted for correlation effects by simply applying the  $-6.0$  kcal/mol correction determined with four waters.



In both cases (Li and K) the fifth and sixth waters add to the waters that are directly coordinated to the metal, but the potassium complex is preferentially stabilized by  $\sim 2$  kcal/mol. The K<sup>+</sup>:18c6(H<sub>2</sub>O)<sub>6</sub> complex can more easily accommodate additional waters because the cation is positioned in the center of the crown, whereas lithium occupies a crowded site very close to one of the macrocycle oxygens. Although calculations on still larger clusters are beyond the scope of the present work, it appears likely that additional waters will continue to shift the balance of eq 1 in favor of potassium and away from lithium.

## Conclusion

Aqueous microsolvation of alkali metal cation/crown ether complexes results in a general decrease in the spread of binding enthalpies compared to values obtained in the absence of water. In the present study, MP2/6-31+G\* calculations on M<sup>+</sup>:18c6-(H<sub>2</sub>O)<sub>n</sub> ( $n \leq 4$ , M = Li through Cs) showed a factor of 4 reduction in  $\Delta H^{298}$  for a model K<sup>+</sup> ↔ M<sup>+</sup> cation exchange reaction after account was taken of basis set superposition errors. Correlation effects were important for describing the interactions of the small cations with the crown and added waters, as well as for describing water–water and water–ether hydrogen bonds. The microsolvated binding enthalpies are in much closer agreement with the aqueous phase values.

**Acknowledgment.** We wish to thank Dr. David Dixon for helpful discussions and Dr. Susan Hill for a critical reading of the manuscript. The Scientific Computing Staff, Office of Energy Research, U.S. Department of Energy, is thanked for a grant of computer time at the National Energy Research Supercomputer Center. This research was supported by the U.S. Department of Energy under Contract DE-AC06-76RLO 1830 (Division of Chemical Sciences, Office of Basic Energy Sciences). The Pacific Northwest National Laboratory is operated by Battelle Memorial Institute.

## References and Notes

- (1) Horwitz, E. P.; Dietz, M. L.; Fisher, D. E. *Solvent Ext. Ion Exch.* **1991**, *9*, 1.
- (2) Glendening, E. D.; Feller, D.; Thompson, M. A. *J. Am. Chem. Soc.* **1994**, *116*, 10657.
- (3) Glendening, E. D.; Feller, D. *J. Am. Chem. Soc.* **1996**, *118*, 6052.
- (4) Garrett, B. C.; Melius, C. F. In *Theoretical and Computational Models for Organic Chemistry*; Ed.; Kluwer Academic Publishers: Amsterdam, 1991.
- (5) Day, P. N.; Jensen, J. H.; Gordon, M. S.; Webb, S. P.; Garmer, D.; Basch, H.; Cohen, D. *J. Chem. Phys.* **1996**, *105*, 1968.
- (6) Chen, W.; Gordon, M. S. *J. Chem. Phys.*, in press.
- (7) Dang, L. X.; Kollman, P. A. *J. Phys. Chem.* **1995**, *99*, 55.
- (8) Dang, L. X. *J. Am. Chem. Soc.* **1995**, *117*, 6954.
- (9) Hehre, W. J.; Ditchfield, R.; Pople, J. A. *J. Chem. Phys.* **1972**, *56*, 2257.
- (10) Clark, T.; Chandrasekhar, J.; Spitznagel, G. W.; Schleyer, P. v. R. *J. Comput. Chem.* **1983**, *4*, 294.
- (11) Hariharan, P. C.; Pople, J. A. *Theor. Chim. Acta* **1973**, *28*, 213.
- (12) Hay, P. J.; Wadt, W. R. *J. Chem. Phys.* **1985**, *82*, 299.
- (13) Frisch, M. J.; Trucks, G. W.; Schlegel, H. B.; Gill, P. M. W.; Johnson, B. G.; Robb, M. A.; Cheeseman, J. R.; Keith, T. A.; Petersson, G. A.; Montgomery, J. A.; Raghavachari, K.; Al-Laham, M. A.; Zakrzewski, V. G.; Ortiz, J. V.; Foresman, J. B.; Cioslowski, J.; Stefanov, B. B.; Nanayakkara, A.; Challacombe, M.; Peng, C. Y.; Ayala, P. Y.; Chen, W.; Wong, M. W.; Andreas, J. L.; Replogle, E. S.; Gomperts, R.; Martin, R. L.; Fox, D. J.; Binkley, J. S.; Defrees, D. J.; Baker, J.; Stewart, J. J. P.; Head-Gordon, M.; Gonzalez, C.; Pople, J. A. *Gaussian 94*, D.3, Gaussian, Inc.: Pittsburgh, PA, 1996.
- (14) Boys, S. F.; Bernardi, F. *Mol. Phys.* **1970**, *19*, 553.
- (15) Xantheas, S. S. *J. Chem. Phys.* **1996**, *104*, 8821.
- (16) Feller, D.; Aprà, E.; Nichols, J. A.; Bernholdt, D. E. *J. Phys. Chem.* **1996**, *105*, 1940.
- (17) Feller, D.; Glendening, E. D.; Kendall, R. A.; Peterson, K. A. *J. Chem. Phys.* **1994**, *100*, 4981.
- (18) Feller, D.; Glendening, E. D.; Woon, D. E.; Feyereisen, M. W. *J. Chem. Phys.* **1995**, *103*, 3526.
- (19) Feller, D.; Thompson, M. A.; Kendall, R. A. To be published.
- (20) Glendening, E. D.; Feller, D. *J. Phys. Chem.* **1995**, *99*, 3060.
- (21) Burke, L. A.; Jensen, J. O.; Jensen, J. L.; Krishnan, P. N. *Chem. Phys. Lett.* **1993**, *206*, 293.
- (22) Tsai, C. J.; Jordan, K. D. *Chem. Phys. Lett.* **1993**, *213*, 181.
- (23) Jensen, J. O.; Krishnan, P. N.; Burke, L. A. *Chem. Phys. Lett.* **1996**, *260*, 499.
- (24) Feller, D. *J. Chem. Phys.* **1992**, *96*, 6104.
- (25) Feyereisen, M. W.; Feller, D.; Dixon, D. A. *J. Phys. Chem.* **1996**, *100*, 2993.
- (26) Xantheas, S. S.; Dunning, T. H., Jr. *J. Chem. Phys.* **1993**, *99*, 8774.
- (27) Dzidic, I.; Kebarle, P. *J. Phys. Chem.* **1970**, *74*, 1466.
- (28) Rodgers, M. T.; Armentrout, P. B. *J. Phys. Chem.* To be published.
- (29) More, M. B.; Glendening, E. D.; Ray, D.; Feller, D.; Armentrout, P. B. *J. Phys. Chem.* **1996**, *100*, 1605.
- (30) Ray, D.; Feller, D.; More, M. B.; Glendening, E. D.; Armentrout, P. B. *J. Phys. Chem.* **1996**, *100*, 16116.
- (31) Thompson, M. A.; Glendening, E. D.; Feller, D. *J. Phys. Chem.* **1994**, *98*, 10465.
- (32) Smetana, A. J.; Popov, A. I. *J. Solution Chem.* **1980**, *9*, 183.